ANNALS of Faculty Engineering Hunedoara
– International Journal of Engineering
Tome XIII [2015] – Fascicule 3 [August]
ISSN: 1584-2673 [CD-Rom; online]
a free-access multidisciplinary publication of the Faculty of Engineering Hunedoara

[1.] Mădălina DUMITRIU, [2.] Marius Alin GHEȚI

EVALUATION OF THE RIDE QUALITY AND RIDE COMFORT IN RAILWAY VEHICLES BASED ON THE INDEX Wz

[1.] University Politehnica of Bucharest, Department of Railway Vehicles, ROMANIA

Abstract: This paper focuses on the evaluation of the ride quality and comfort during the vertical vibrations in the railway vehicles generated by the track irregularities, where this evaluation applies the ride index Wz method. The ride index Wz is calculated via certain applications of numerical simulation, based on which the impact of the velocity and of the suspension features upon the ride quality and ride comfort is analyzed. The derived results emphasize a series of attributes of the dynamic behaviour of the vehicle, as well as the possibilities of increasing the ride quality and comfort by means of an appropriate selection of the damping of the secondary suspension.
Keywords: railway vehicle, vertical vibrations, ride quality, ride comfort, track irregularities, suspension, damping

1. INTRODUCTION

The ride quality and the ride comfort, along with the safety, vehicle stability and the vehicle curve-negotiation capability are the utmost criteria of evaluating the dynamic performance of the railway vehicle [1].

The ride quality can be defined as the capacity of the vehicle to fulfill the transport requirements from the perspective of vibrations level of exposure, depending on the vehicle type, number of trips, goods or the engine operating staff. As for the ride comfort, its evaluation requires the effect of the mechanical vibrations upon the human body be considered.

To evaluate the dynamic performance of the railway vehicles, numerous methods have been developed and included in standards or normative acts pertinent to the railway applications. Regulations concerning the evaluation of the dynamic behaviour of the vehicle in terms of the ride quality are thus enumerated in the UIC 518 [2] leaflet and in EN 14363 [3], the European standard of railway applications. To have the evaluation of the comfort during vibrations carried out, ISO 2631-based procedures [4] are often used. For that reason, the International Standardization Organization (ISO) has revised the ISO 2631 standard, in order to evaluate the exposure to the vibrations conveyed to the human body [5-7]. During the International Union of Railways (UIC), the European Committee for Standardization (CEN) and the International Organization for Standardization (ISO), the standards of evaluating the ride comfort of the railway vehicles based on the ISO 2631 standard have been established, namely ERRI [8, 9], UIC 513R [10], ENV 12299 [11], BS 6841 [12] and ISO 10056 [13].

A method that is applied for both calculating the ride quality and ride comfort to the railway vehicles is the Ride Index Wz method. Sperling [14, 15] was the one to introduce this method in Germany in the mid of last century and it was later used by other railway administrations. Currently, this method is only used in Sweden, for Europe, and in Asia, i.e. China or India.

The advantage and clarity of the Ride Indez Wz method comes from the fact that its implementation leads to a number with a precise signifiance, being thus easily explained. Since it is determined as a function of the level in the vehicle vibrations, the ride index Wz supplies information on the dynamic behaviouur of the vehicle, which makes possible the identification of certain solutions to improve the dynamic performance of the vehicle in terms of the ride quality and ride comfort [16].

The methods of evaluating this dynamic performance are to be found in a large number of studies in the relevant literature. For instance, there are the studies attempting to establish a correlation between the methods of evaluating the comfort during vibrations [17, 18]. There is also an extensive research relying on the methods of evaluating the dynamic performance, aiming to study the influence of certain vehicle parameters, of the track's and of the conditions of exploitation upon the ride quality or ride comfort [19 - 25]. Similarly, applications of the comfort evaluation methods are included in experimental studies [26, 27] or in studies focusing on improving the dynamic performance in the railway vehicles [28, 29].

The paper herein applies the ride index Wz method to evaluate the ride quality and ride comfort on the vertical direction of a four-axle vehicle. This is represented by a mechanical model, ‚rigid body' type, with 6 degrees of freedom corresponding to the bounce

and pitch movements of the carbody and the two bogies. To calculate the ride index Wz, there will be adopted the hypothesis that the track vertical irregularities, which induce vibrations to the vehicle, describes a stochastic stationary process that can be defined via the power spectral density. A numerical model that is representative for the passenger cars will be considered. While using the numerical simulations, the influence of the velocity and of the suspension characteristics on the size of the ride index Wz is being examined. The results thus found are pointing out at a series of properties of the dynamic behaviour of the vehicle, as well as the possibilities of improving the ride quality and ride comfort by an appropriate selection of the suspension parameters.

2. THE RIDE INDEX Wz METHOD

To assess the ride quality, the ride index Wz is calculated with the relation below

$$W_z = 0.896 \cdot \sqrt[10]{\frac{a^3}{f}}, \tag{1}$$

where a stands for the amplitude of the carbody acceleration in cm/s^2 and f is the excitation frequency; for the ride comfort, the following relation is in use

$$W_z = 0.896 \cdot \sqrt[10]{\frac{a^3}{f} F(f)}, \tag{2}$$

that includes the weighting factor $F(f)$, as defined in the table 1.

This factor corrects the value of the acceleration in dependence on the frequency, in order to take into account the sensitivity of the human body to vibrations. The equations in the table 1 show the fact that the human sensitivity to vibrations depends on their direction and frequency.

Table 1. The acceleration weighting factor

Direction	Computation relation	Applicability domain
Vertical	$F(f) = 0.325f$	$0.5 < f < 5.9$ Hz
	$F(f) = 400/f$	$5.9 < f < 20$ Hz
	$F(f) = 1$	$f > 20$ Hz
Horizontal	$F(f) = 0.8f$	$0.5 < f < 5.9$ Hz
	$F(f) = 650/f$	$5.9 < f < 26$ Hz
	$F(f) = 1$	$f > 26$ Hz

An observation should be made, namely that the relations (1) and (2) are valid only if the vibration is harmonic. In reality, the vibrations of the vehicle are stochastic and, hence, the practice will use the relation below

$$W_z = 10\sqrt{\int_{0,5}^{30} a^3(f) \cdot B^3(f) df}, \tag{3}$$

where $a^3(f)$ is the amplitude of the spectral component of the carbody acceleration, corresponding to the oscillation frequency f, and $B(f)$ is the weighting factor of the acceleration (see Figure 1).

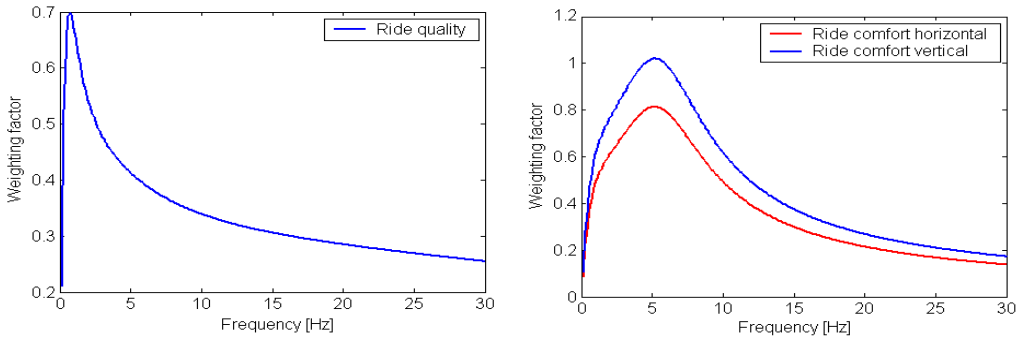

Figure 1. Weighting factor $B(f)$.

The relation (3) is applied on the supposition that the spectrum of the accelerations is a continuous function of frequency and the energy of vibrations is limited to the interval between 0.5 and 30 Hz.

The weighting factor $B(f)$ is calculated differentially, as such:

- for the ride quality

$$B(f) = 1.14 \sqrt{\frac{\left[\left(1-0.056f^2\right)^2 + \left(0.645f\right)^2\right] \cdot 3.55f^2}{\left[\left(1-0.252f^2\right)^2 + \left(1.547f - 0.00444f^3\right)^2\right] \cdot \left(1+3.55f^2\right)}}; \tag{4}$$

- for the ride comfort

$$B(f)=k\sqrt{\frac{1.911f^2+\left(0.25f^2\right)^2}{\left(1-0.277f^2\right)^2+\left(1.563f-0.0368f^3\right)^2}}, \quad (5)$$

where $k=0.588$ for the carbody vibrations in the vertical plan and $k=0.737$ for the horizontal vibrations.

The significance of the ride index Wz for evaluating the ride quality is mentioned in table 2; table 3 describes the relation between the comfort index and the sensitivity to the vertical and horizontal vibrations.

Table 2. Ride evaluation scales – ride quality.

Ride index Wz	Ride quality
1.0	Very good
2.0	Good
3.0	Satisfactory
4.0	Acceptable for running
4.5	Not acceptable for running
5.0	Dangerous

Table 3. Ride evaluation scales – ride comfort.

Ride index Wz	Ride comfort
1.0	Just noticeable
2.0	Clearly noticeable
2.5	More pronounced but not unpleasant
3.0	Strong, irregular, but still tolerable
3.5	Very irregular
3.5	Extremely irregular, unpleasant, annoying; prolonged exposure intolerable
4.0	Extremely unpleasant; prolonged exposure harmful

3. THE MECHANICAL MODEL AND THE MOTION EQUATION OF THE VEHICLE

The mechanical model of the vehicle for the study of the vertical vibrations is featured in the figure 2 [30]. It is about a four-axle vehicle with two level suspension, which travels at a constant velocity V along a perfectly rigid track that impresses displacements to the vehicle via the axles, due to the vertical irregularities. These irregularities are described against each axle by means of the functions f_j, for $j=1...4$.

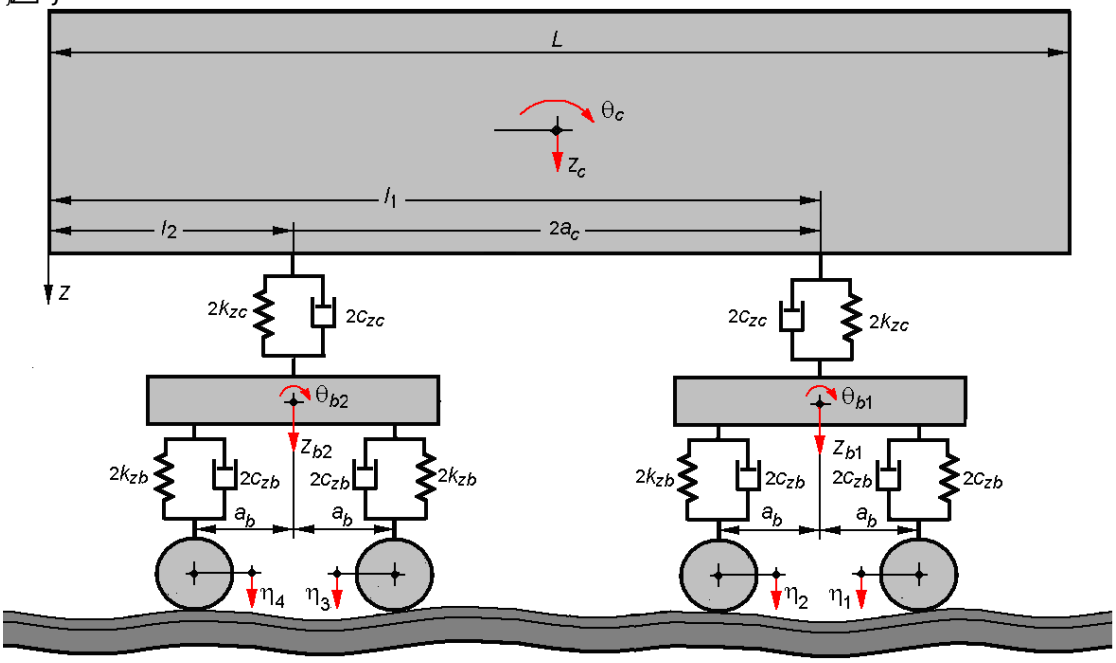

Figure 2. The mechanical model of the vehicle

The vehicle model consists of rigid bodies that represent the vehicle carbody, the suspended massed of the two bogies and four axles, connected among them by Kelvin-Voigt type systems, which models the suspension levels.

The carbody vibration modes are the bounce z_c and the pitch θ_c, while the carbody inertia compared to these is represented by the mass m_c and the inertia moment J_c. The bogies have two degrees of freedom, namely the bounce z_{bi} and the pitch θ_{bi}, for $i=1, 2$. Each bogie has the mass m_b and the inertia moment J_b.

The elastic and damping elements of the secundary suspension of each bogie are modelled via a Kelvin-Voigt system that operates during translation, with the elastic constant $2k_{zc}$ and the damping constant $2c_{zc}$. The primary suspension corresponding to an axle is modelled via a Kelvin-Voigt system, operating during translation, with the elastic constant $2k_{zb}$ and the damping constant $2c_{zb}$.

The equations of the bounce and pitch carbody motions are as follows:

$$m_c\ddot{z}_c+2c_{zc}(2\dot{z}_c-\dot{z}_{b1}-\dot{z}_{b2})+2k_{zc}(2z_c-z_{b1}-z_{b2})=0; \quad (6)$$

$$J_c\ddot{\theta}_c+2a_cc_{zc}(2a_c\dot{\theta}_c-\dot{z}_{b1}+\dot{z}_{b2})+2a_ck_{zc}(2a_c\theta_c-z_{b1}+z_{b2})=0, \quad (7)$$

where $2a_c$ is the carbody wheelbase.

The equation of the bounce motion for the front bogie is

$$m_b\ddot{z}_{b1}+2c_{zc}(\dot{z}_{b1}-\dot{z}_c-a_c\dot{\theta}_c)+2k_{zc}(z_{b1}-z_c-a_c\theta_c)++2c_{zb}(2\dot{z}_{b1}-\dot{\eta}_1-\dot{\eta}_2)+2k_{zb}(2z_{b1}-\eta_1-\eta_2)=0 \quad (8)$$

and for the rear one writes as

$$m_b\ddot{z}_{b2}+2c_{zc}(\dot{z}_{b2}-\dot{z}_c+a_c\dot{\theta}_c)+2k_{zc}(z_{b2}-z_c+a_c\theta_c)+2c_{zb}(2\dot{z}_{b2}-\dot{\eta}_3-\dot{\eta}_4)+2k_{zb}(2z_{b2}-\eta_3-\eta_4)=0 \quad (9)$$

Similarly, the equations of the pitch motion for the two bogies are:

- for the front bogie

$$J_b\ddot{\theta}_{b1}+2a_bc_{zb}(2a_b\dot{\theta}_{b1}-\dot{\eta}_1+\dot{\eta}_2)+2a_bk_{zb}(2a_b\theta_{b1}-\eta_1+\eta_2)=0\,; \quad (10)$$

- for the rear bogie

$$J_b\ddot{\theta}_{b2}+2a_bc_{zb}(2a_b\dot{\theta}_{b2}-\dot{\eta}_3+\dot{\eta}_4)+2a_bk_{zb}(2a_b\theta_{b2}-\eta_3+\eta_4)=0\,, \quad (11)$$

where $2a_b$ represents the bogie wheelbase.

The bounce and pitch carbody motions are noticed to be coupled by the bounce motion of the bogies. Nevertheless, they can be decoupled following a convenient selection of the coordinates for the motions and an appropriate processing of the first four equations. To this purpose, the following changes in the coordinates are made:

- for the symmetrical motions

$$z_c^+=z_c\,;\ 2z_b^+=z_{b1}+z_{b2}\,; \quad (12)$$

- for the antisymmetrical motions

$$z_c^-=\theta_c\,;\ 2z_b^-=z_{b1}-z_{b2}\,. \quad (13)$$

According to the latest notations, the relations (6) – (9) write as:

$$m_c\ddot{z}_c^++4c_{zc}(\dot{z}_c^+-\dot{z}_b^+)+4k_{zc}(z_c^+-z_b^+)=0\,; \quad (14)$$

$$J_c\ddot{z}_c^-+4a_cc_{zc}(a_c\dot{z}_c^--\dot{z}_b^-)+4a_ck_{zc}(a_cz_c^--z_b^-)=0\,; \quad (15)$$

$$m_b\ddot{z}_b^++2c_{zc}(\dot{z}_b^+-\dot{z}_c^+)+2_{zc}(z_b^+-z_c^+)+4c_{zb}(\dot{z}_b^+-\dot{\eta}^+)+4k_{zb}(z_b^+-\eta^+)=0\,; \quad (16)$$

$$m_b\ddot{z}_b^-+2c_{zc}(\dot{z}_b^--a_c\dot{z}_c^-)+2k_{zc}(z_b^--a_cz_c^-)+4c_{zb}(\dot{z}_b^--\dot{\eta}^-)+4k_{zb}(z_b^--\eta^-)=0\,, \quad (17)$$

where

$$\eta^+=\frac{\eta_1+\eta_2+\eta_3+\eta_4}{4}\,;\ \eta^-=\frac{\eta_1+\eta_2-\eta_3-\eta_4}{4}\,, \quad (18)$$

represent the functions corresponding to the excitation modes due to the motions of symmetrical and antisymmetrical bounce of the plans of the vehicle's axles (see Figure 3) [31].

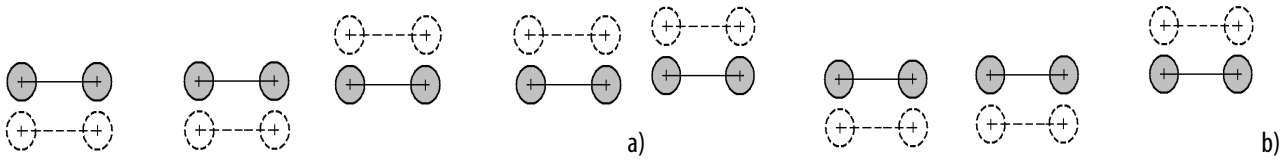

Figure 3. The motion modes of the planes of the vehicle's axles: (a) symmetrical bounce; (b) antisymmetrical bounce.

Written as above, the motion equations can be further classiffied into two independent systems of two equations each, describing the symmetrical (14 and 16) and antisymmetrical motions of the vehicle (15 and 17).

4. THE RESPONSE FUNCTIONS OF THE VEHICLE

Further on, it is considered that the track vertical irregularities are in a harmonic shape with the wavelength Λ and amplitude η_0. With the reference to each axle, the vertical irregularities of the track can be written as

$$\eta_{1,2}(x)=\eta_0\cos\frac{2\pi}{\Lambda}(x+a_c\pm a_b)\,;\ \eta_{3,4}(x)=\eta_0\cos\frac{2\pi}{\Lambda}(x-a_c\mp a_b)\,, \quad (19)$$

where $x=Vt$ is the coordinate of the car body centre.

The functions η_j (with $j=1\ldots4$) can be expressed as time harmonic functions

$$\eta_{1,2}(x)=\eta_0\cos\omega\left(t+\frac{a_c\pm a_b}{V}\right)\,;\ \eta_{3,4}(x)=\eta_0\cos\omega\left(t-\frac{a_c\mp a_b}{V}\right), \quad (20)$$

in which $\omega=2\pi V/\Lambda$ means the angular frequency induced by the track excitation, while the corresponding frequency is $f=V/\Lambda$. As for the vehicle response, this is assumed to be harmonic, with the same frequency as the track excitation induced frequency. The coordinates describing the symmetrical and antisymmetrical motions of the vehicle are written under the general form as

$$z_c^{\pm}(t)=Z_c^{\pm}\cos(\omega t+\alpha^{\pm});\ z_b^{\pm}(t)=Z_b^{\pm}\cos(\omega t+\beta^{\pm}), \tag{21}$$

where $Z_c^{\pm}$ stands for the amplitude of the carbody movement, $Z_b^{\pm}$ - the amplitude of the bogie movement and $\alpha^{\pm}$ and $\beta^{\pm}$ are the displacements of the coordinates $z_c^{\pm}$ and $z_b^{\pm}$, in relation to the track vertical irregularities against the centre of the vehicle.

In addition, the complex values associated with the real ones, for $i^2=-1$:

- for the track vertical irregularities with the reference to the axles

$$\overline{\eta}_j(t)=\overline{\eta}_j e^{i\omega t}; \tag{22}$$

- for the coordinates of the vehicle motions

$$\overline{z}_c^{\pm}=\overline{Z}_c^{\pm}e^{i\omega t};\ \overline{z}_b^{\pm}=\overline{Z}_b^{\pm}e^{i\omega t}, \tag{23}$$

where the complex amplitudes of the track irregularities with the reference to the axles are in the form of

$$\overline{\eta}_{1,2}=\eta_0 e^{i\omega\left(t+\frac{a_c\pm a_b}{V}\right)};\ \overline{\eta}_{3,4}=\eta_0 e^{i\omega\left(t-\frac{a_c\mp a_b}{V}\right)}, \tag{24}$$

while the complex amplitude of the coordinates $z_c^{\pm}$ şi $z_b^{\pm}$ writes as

$$\overline{Z}_c^{\pm}=z_c^{\pm}e^{i\alpha^{\pm}};\ \overline{Z}_b^{\pm}=z_b^{\pm}e^{i\beta^{\pm}}. \tag{25}$$

Likewise, starting from the relations (18), the functions describing the symmetrical and antisymmetrical excitation modes, induced by the track vertical irregularities can be written as

$$\overline{\eta}^{+}(t)=\frac{\overline{\eta}_1+\overline{\eta}_2+\overline{\eta}_3+\overline{\eta}_4}{4}e^{i\omega t}=\frac{1}{4}\eta_0\overline{H}_f^{+}e^{i\omega t}; \tag{26}$$

$$\overline{\eta}^{-}(t)=\frac{\overline{\eta}_1+\overline{\eta}_2-\overline{\eta}_3-\overline{\eta}_4}{4}e^{i\omega t}=\frac{1}{4}\eta_0\overline{H}_f^{-}e^{i\omega t}, \tag{27}$$

where

$$\overline{H}_f^{+}=e^{i\omega\frac{a_c+a_b}{V}}+e^{i\omega\frac{a_c-a_b}{V}}+e^{-i\omega\frac{a_c-a_b}{V}}+e^{-i\omega\frac{a_c+a_b}{V}}; \tag{28}$$

$$\overline{H}_f^{-}=e^{i\omega\frac{a_c+a_b}{V}}+e^{i\omega\frac{a_c-a_b}{V}}-e^{-i\omega\frac{a_c-a_b}{V}}-e^{-i\omega\frac{a_c+a_b}{V}} \tag{29}$$

are the geometric filtering characteristics of these excitation modes. The geometric filtering effect is introduced by the carbody wheelbase and the bogie wheelbase, with a selective nature, depending on the velocity [32].

The differential equations of motion (14 - 17) will turn into algebraic equations in the form of:

$$-\omega^2\overline{Z}_c^{+}+4\alpha_{zc}(\overline{Z}_c^{+}-\overline{Z}_b^{+})=0; \tag{30}$$

$$-\omega^2 J_c\overline{Z}_c^{-}+4a_c\alpha_{zc}(a_c\overline{Z}_c^{-}-\overline{Z}_b^{-})=0; \tag{31}$$

$$-\omega^2 m_b\overline{Z}_b^{+}+2\alpha_{zc}(\overline{Z}_b^{+}-\overline{Z}_c^{+})+4\alpha_{zb}\overline{Z}_b^{+}=4\alpha_{zb}\overline{\eta}^{+}; \tag{32}$$

$$-\omega^2 m_b\overline{Z}_b^{-}+2\alpha_{zc}(\overline{Z}_b^{-}-a_c\overline{Z}_c^{-})+4\alpha_{zb}\overline{Z}_b^{-}=4\alpha_{zb}\overline{\eta}^{-}, \tag{33}$$

with the following notations:

$$\alpha_{zc}=i\omega c_{zc}+k_{zc};\ \alpha_{zb}=i\omega c_{zb}+k_{zb}. \tag{34}$$

There can also be determined the carbody response functions of the vehicle to the excitations coming from the track vertical irregularities.

The response function of the carbody movement in a random abscissa point *x* (for $0\le x\le L$, where *L* is the carbody length) corresponding to the excitation frequency *f* writes as

$$\overline{H}_c(f,x)=\overline{H}_{z_c}(f)+\left(\frac{L}{2}-x\right)\overline{H}_{\theta_c}(f), \tag{35}$$

in which $\overline{H}_{z_c}(f)$, $\overline{H}_{\theta_c}(f)$ are the response functions corresponding to the bounce (z_c) and pitch motions (θ_c) of the carbody, calculated as below

$$\overline{H}_{z_c}(f)=\frac{\overline{Z}_c^{+}}{\overline{\eta}_0};\ \overline{H}_{\theta_c}(f)=\frac{\overline{Z}_c^{-}}{\overline{\eta}_0}. \tag{36}$$

The relation (35) can be customized for three reference points at the carbody centre and above the two bogies. Thus, the response function of the movement at the centre is

$$\overline{H}_{cm}(f,L/2)=\overline{H}_{z_c}(f), \tag{37}$$

whereas above the two bogies writes as

$$\overline{H}_{cbi}(f,l_i)=\overline{H}_{z_c}(f)\pm a_c\overline{H}_{\theta_c}(f), \text{ for } i=1,2. \tag{38}$$

where the distances l_i set the position of the carbody supporting points on the secondary suspension (v. Figure 2).

5. THE VEHICLE DYNAMIC RESPONSE TO THE TRACK STOCHASTIC IRREGULARITIES

Further on, the track vertical irregularities are considered to represent a stationary stochastic process, which can be described via the power spectral density. The theoretical curve of the power spectral density is representative for the average statistical properties of the European railway, as in the relation [33]

$$S(\Omega)=\frac{A\Omega_c^2}{(\Omega^2+\Omega_r^2)(\Omega^2+\Omega_c^2)}, \tag{39}$$

where Ω is the wavelength, $\Omega_c = 0.8246$ rad/m, $\Omega_r = 0.0206$ rad/m, and A is a coefficient depending on the track quality. For a high level quality track, $A = 4.032\cdot10^{-7}$ radm, whereas for a low level quality, the coefficient A is $1.080\cdot10^{-6}$ radm.

As a function of the angular frequency $\omega = V\Omega$, the power spectral density of the track irregularities can be written as in the general relation

$$G(\omega)=S(\omega/V). \tag{40}$$

What results is the power spectral density of the track irregularities in the form of

$$G(\omega)=\frac{A\Omega_c^2V^3}{[\omega^2+(V\Omega_c)^2][\omega^2+(V\Omega_r)^2]} \tag{41}$$

or

$$G(f)=\frac{A\Omega_c^2V^3}{[(2\pi f)^2+(V\Omega_c)^2][(2\pi f)^2+(V\Omega_r)^2]}. \tag{42}$$

Starting from the response functions of the vehicle carbody and the spectrum of the track irregularities, the power spectral density of the carbody vertical movement is calculated, as in the general relation

$$G_c(f,x)=G(f)\left|\overline{H}_c(f,x)\right|^2. \tag{43}$$

Upon applying the above equation, the result will be the power spectral density in the reference point at the carbody centre and in the points above the bogies, respectively:

$$G_{cm}(f,L/2)=G(f)\left|\overline{H}_{cm}(f,L/2)\right|^2; \tag{44}$$

$$G_{cb_1}(f,l_i)=G(f)\left|\overline{H}_{cb_i}(f,l_i)\right|^2. \tag{45}$$

The power spectral density of the carbody acceleration is established from the below equation:

$$G_{ca}(f,x)=\omega^4G(f)\left|\overline{H}_c(f,x)\right|^2, \tag{46}$$

which can be also written for the three reference carbody points by a suitable replacement of the response functions with the particular relations (37) and (38).

Based on vehicle dynamic response, expressed in the form of the power spectral density of the carbody acceleration, the root mean square acceleration can be further calculated.

$$a=\sqrt{\frac{1}{\pi}\int_0^\infty G_{ca}(f,x)df}. \tag{47}$$

6. NUMERICAL APPLICATION

This section describes the results of the numerical simulations regarding the influence of the velocity and of the suspension characteristics upon the ride quality and ride comfort, evaluated on the basis of the ride index Wz. The parameters of numerical simulation are featured in the table 4, as representative for a passenger car. Figure 4 shows the distribution of the ride quality index along the carbody

Table 4. The parameters of the vehicle numerical model

Carbody mass	$m_c = 34000$ kg
Suspended mass of the bogie	$m_b = 3200$ kg
Carbody inertia moment	$J_c = 1963840$ kg·m^2
Bogie inertia moment	$J_b = 2048$ kg·m^2
Carbody wheelbase	$2a_c = 19$ m
Bogie wheelbase	$2a_b = 2.56$ m
Constants of the secondary suspension	$2k_{zc} = 1.2$ MN/m
	$2c_{zc} = 34.44$ kNs/m
Constants of the primary suspension	$4k_{zb} = 4.4$ MN/m
	$4c_{zb} = 52.21$ kNs/m

(diagram (b)) for velocities ranging between 20 and 300 km/h during the vehicle circulation on a good quality track ($A = 4.032 \cdot 10^{-7}$ radm), with vertical irregularities represented by the power spectral density, as in relation (41). Both diagrams exemplify the symmetrical distribution of the ride index Wz against the carbody centre and the fact that this index has different variation laws depending on the velocity. Generally speaking, the ride index Wz rises along with the velocity, but this increase is not uniform, due to the geometric filtering effect coming from the vehicle wheelbases [32].

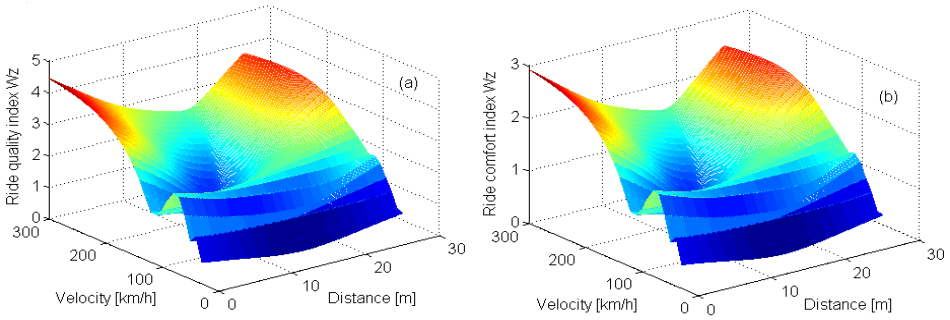

Figure 4. The distribution of the ride index Wz along the vehicle carbody: (a) ride quality index; (b) ride comfort index.

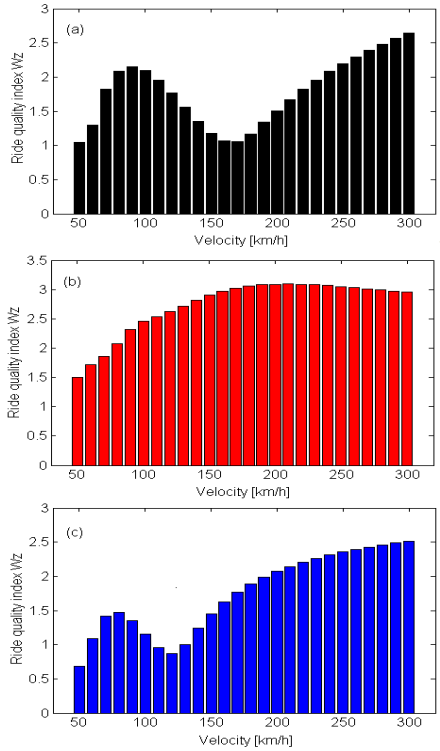

Figure 5. Ride quality index: (a) carbody centre; (b) above the front bogie; (c) above the rear bogie.

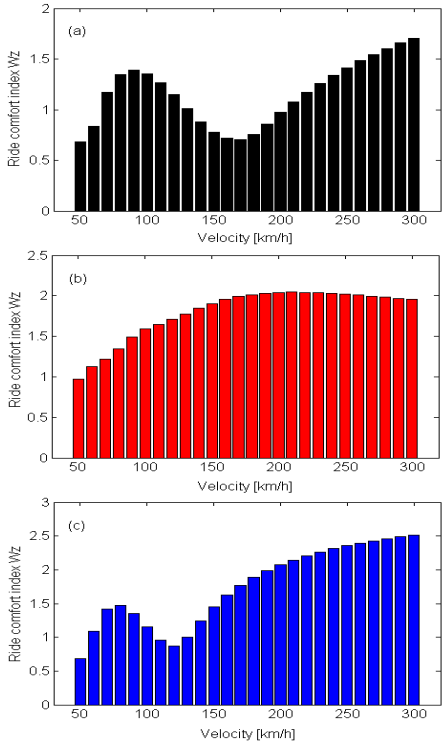

Figure 6. Ride comfort index: (a) carbody centre; (b) above the front bogie; (c) above the rear bogie.

In general terms, the ride index Wz is smaller at the carbody centre and higher against the two bogies and towards its ends. This fact is also made visible in the diagrams in Figure 5 and Figure 6, where the values of the ride index Wz in all three reference carbody points – at the centre and above the two bogies – are introduced. In addition, the diagrams (b) and (c) are included in the Figure 5 and Figure 6, where they display the different vibration carbody behaviour against the two bogies. Local minimum values of the ride index Wz can be noticed for certain velocities, by reason of the geometric filtering effect. Therefore, the ride index Wz is minimum at speed of 170 km/h at the carbody centre, due to the geometric filtering effect for the symmetrical bounce mode of the axles' plans. Another minimum value of this index is present against the rear bogie for the speed of 120 km/h, as a result of the cumulated filtering effect coming from the symmetrical and antisymmetrical bounce mode of the axles' plans.

Further on, the damping ratios of the two suspension levels are introduced, in order to examine the influence of the suspension characteristics upon the ride quality and ride comfort, as

$$\zeta_{zc} = \frac{4c_{zc}}{2\sqrt{4k_{zc}m_c}};\ \zeta_{zb} = \frac{4c_{zb}}{2\sqrt{4k_{zb}m_b}}. \tag{48}$$

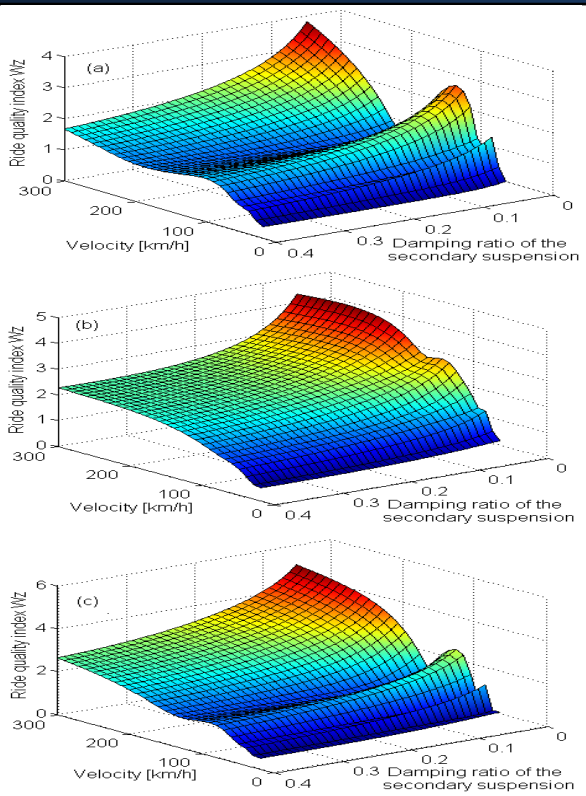

Figure 7. Influence of the secondary suspension damping upon the ride quality index: (a) carbody centre; (b) above the front bogie; (c) above the rear bogie.

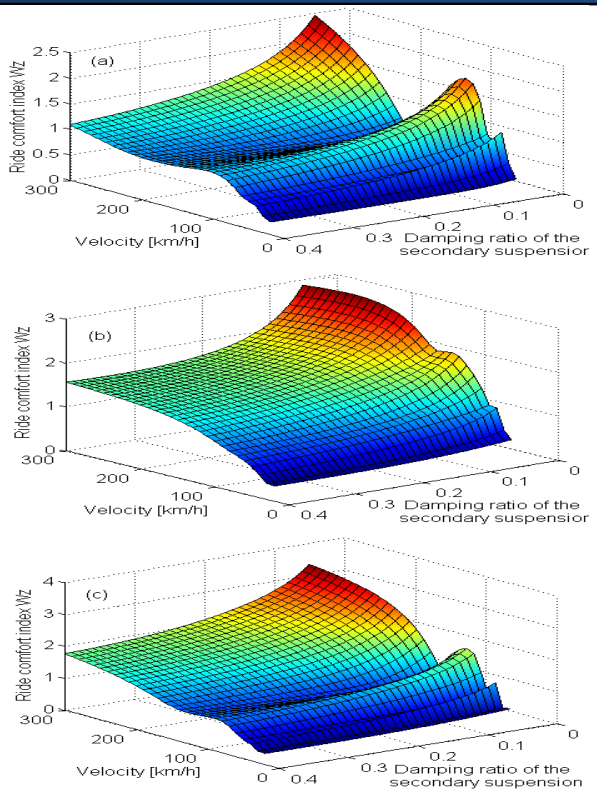

Figure 8. Influence of the secondary suspension damping upon the ride comfort index: (a) carbody centre; (b) above the front bogie; (c) above the rear bogie.

Table 5. The damping ratio of the secondary suspension minimizing the ride index Wz.

Reference point	Ride quality index			Ride comfort index		
	V [km/h]	Wzmin	ζ_{zc}	V [km/h]	Wzmin	ζ_{zc}
carbody centre	110	1.31	0.34	130	0.87	0.32
	120	1.24	0.26	140	0.82	0.24
	130	1.15	0.18	150	0.77	0.17
	140	1.07	0.11	160	0.71	0.09
	150	1.05	0.15	170	0.70	0.13
	160	1.08	0.22	180	0.72	0.19
	170	1.12	0.28	190	0.75	0.25
	180	1.17	0.33	200	0.78	0.29
	190	1.21	0.37	210	0.81	0.33
				220	0.84	0.36
				230	0.86	0.39
above the front bogie	260	2.24	0.39	240	0.39	1.50
	270	2.25	0.38	250	0.38	1.50
	280	2.25	0.37	260	0,37	1.15
	290	2.26	0.36	270	0,36	1.52
	300	2.26	0.35	280	0,35	1.52
				290	0,34	1.53
				300	0,33	1.53
above the rear bogie	100	1.49	0.35	180	0.32	1.00
	110	1.37	0.20	190	0.19	0.91
	120	1.30	0.18	200	0.16	0.85
	130	1.34	0.22	210	0.21	0.88
	140	1.44	0.35	220	0.31	0.95
				230	0.39	1.01

The diagrams in Figure 7 show the ride quality index Wz, while the ride comfort index Wz is in the Figure 8, calculated for various values of the damping ratio of the secondary suspension, found within the interval of 0.05 . . . 0.4. A mention should be made that the values in table 4 remain the same for the other parameters of the vehicle numerical model. As a matter of fact, an increase in the damping ratio of the secondary suspension leads to a higher ride quality and ride comfort. More than that, as a function of velocity, a damping value taking to minimum valus of the ride index Wz can be identified, a value that depends on the position of the carbody reference point – at centre or above the bogies (see table 5). In effect, a higher damping of the secondary suspension, up to a certain value, translates as an improvement of the ride quality and ride comfort, respectively. Once this value is exceeded,

the index Wz starts going up again. It needs to specify that, as a principle, there is a value of the secondary suspension damping minimizing the ride index Wz for any velocity; but herein, for certain speeds, this value is higher than the superior limit of the interval adopted for ζ_{zc}.

Table 6. The damping ratio of the primary suspension minimizing the ride index Wz

Reference point	Ride quality index		Ride comfort index	
	ζ_{zb}	Wz	ζ_{zb}	Wz
carbody centre	0.05	2.77	0.05	1.79
	0.4	2.53	0.4	1.63
above the front bogie	0.05	3.11	0.05	2.06
	0.4	2.81	0.4	1.86
above the rear bogie	0.05	3.99	0.05	2.62
	0.4	3.70	0.4	2.42

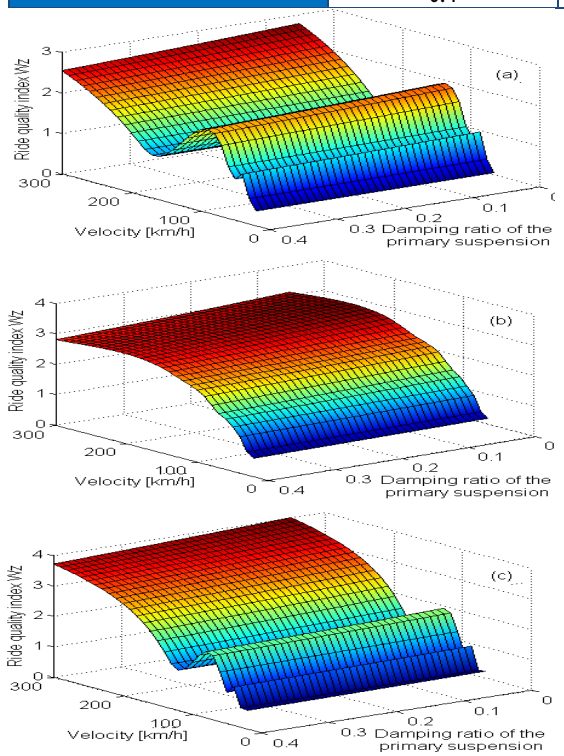

Figure 9. Influence of the primary suspension damping upon the ride quality index: (a) carbody centre; (b) above the front bogie; (c) above the rear bogie.

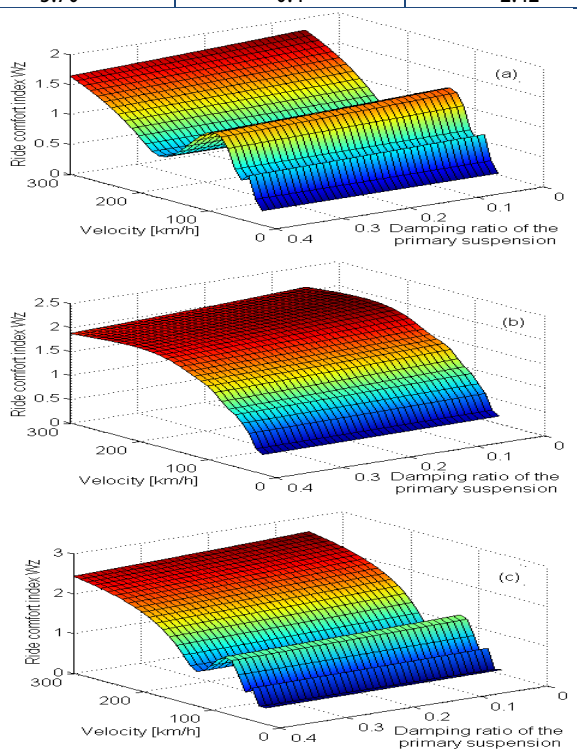

Figure 10. Influence of the primary suspension damping upon the ride comfort index: (a) carbody centre; (b) above the front bogie; (c) above the rear bogie.

The influence of the primary suspension damping upon the ride quality index Wz and ride comfort index Wz is shown in the diagrams in Figure 9 and Figure 10, respectively, taking into account values of ζ_{zb} between 0.05 and 0.4. The increase of the primary suspension damping will lead to a uniform decrease of the ride index Wz, yet not significant. At the velocity of 300 km/h, the increment of the primary suspension damping ratio from 0.05 to 0.4 will have the values corresponding to the ride index Wz featured in the table 6. For an 8 time - increase of ζ_{zb}, the reduction of the ride index Wz does not exceed 10%.

The lower influence of the primary suspension damping compared to the one of the secondary's can be explained by the fact that the bogie mass interposes between the two suspension levels, a mass whose inertia reduces the efficiency of the damping of the first suspension level.

7. CONCLUSIONS

The purpose of this paper was to evaluate the ride quality and ride comfort of the railway vehicles in relation to the vibrations generated during the running on a track with vertical irregularities. To this end, the ride index Wz has been established in three reference points of the carbody – at its centre and above the two bogies, by means of certain applications of numerical simulation, developed via the Matlab programming environment.

The results point out, at the one hand, at a series of characteristics of the vehicle dynamic behaviour in the vertical plan and, on the other hand, at the influence of the velocity and suspension parameters on the ride quality and the ride comfort.

Another conclusion is that, irrespective of the velocity, the ride index Wz is generally smaller at the carbody centre and goes up against the bogies. Similarly, the asymmetry of the vibrations behaviour of the vehicle carbody has been noticed in the reference points located above the two bogies. The geometric filtering effect, coming from the distance between the axles, is another

characteristic of this dynamic behaviour that has been emphasized on. In this context, the selective nature of this effect has been featured – as a function of velocity – which explains why the ride index Wz does not have a uniform increase along the velocity.

In terms of the influence of the suspension parameters on the ride quality and ride comfort, the conclusion is that a value of the secondary damping of the vertical suspension minimizing the ride index Wz can be identified, regardless of the velocity behaviour. This value depends on the position of the carbody reference point. Similarly, an increase in the primary suspension damping will not lead to a sensible improvement in the ride quality and ride comfort.

REFERENCES

[1.] Garg, V.K., Dukkipati, R.V., Dynamics of railway vehicle systems, Academic Press, New York, 1984.
[2.] UIC 518 Leaflet - 4th edition - Sept. 2009. Testing and approval of railway vehicles from the point of view of their dynamic behaviour – Safety – Track fatigue – Running behaviour.
[3.] EN 14363 / 2013. Railway applications - Testing and Simulation for the acceptance of running characteristics of railway vehicles - Running behaviour and stationary tests.
[4.] ISO 2631-4, Mechanical vibration and shock-evaluation of human exposure to whole-body vibration. Part 4: Guidelines for the evaluation of the effects of vibration and rotational motion on passenger and crew comfort in fixed guideway transport systems, 2001.
[5.] ISO 2631(E), Guide for the evaluation of human exposure to whole-body vibration, 1974.
[6.] ISO 2631-1, Mechanical vibration and shock-evaluation of human exposure to whole-body vibration. Part 1: General requirements, 1985.
[7.] ISO 2631-4, Mechanical vibration and shock-evaluation of human exposure to whole-body vibration. Part 4: Guidelines for the evaluation of the effects of vibration and rotational motion on passenger and crew comfort in fixed guideway transport systems, 2001.
[8.] B153/RP1-RP20, Application of ISO Standard to railway vehicles, 1981-1993.
[9.] B153/RP21, Application of ISO Standard to railway vehicles: Comfort Index Nmv Comparison with the ISO/SNCF Comfort Note.
[10.] UIC 513 R, Guidelines for evaluating passenger comfort in relation to vibration in railway vehicle, International Union of Railways, 1994.
[11.] ENV 12299, Railway applications ride comfort for passengers measurement and evaluation, 1997.
[12.] BS 6841, Guide to measurement and evaluation of human exposure to whole-body mechanical vibration and repeated shock, 1987.
[13.] ISO 10056, Mechanical vibration-measurement and analysis of whole-body vibration to which passengers and crew are exposed in railway vehicles, 2001.
[14.] Sperling, E., Verfahren zur beurteilung der laufeigenschaften von eisenbahnwesen, Organ f.d. Fortschritte des Eisenbahnwesens, Vol. 12, 1941, pp. 176–187.
[15.] Sperling, E., Betzhold, C., Beitrag zur beurteilung des fahrkomforts in schienenfahrzeugen, Glasers Annalen, Vol. 80, 1956, pp. 314–320.
[16.] Sebeşan, I., Dinamica vehiculelor feroviare (Dynamic of the railway vehicles), Ed. Matrix Rom, Bucureşti, 2011.
[17.] Kim, Y.G., Kwon, H.B., Kim, S.W., Park, C.K. Park, T.W., Correlation of ride comfort evaluation methods for railway vehicles, Proceedings of the Institution of Mechanical Engineers, Part F: Journal of Rail and Rapid Transit, 217: 73, 2003.
[18.] Yoo, W.S., Lee, C.H., Jeong,W.B., Kim, S.H., Development and application of new evaluation system for ride comfort and vibration on railway vehicles, Journal of Mechanical Science and Technology, Vol 19, no.7, 2005, pp. 1469-1477.
[19.] Kang, J.S., Choi, Y.S., Choe, K., Whole-body vibration analysis for assessment of railway vehicle ride quality, Journal of Mechanical Science and Technology, Vol. 25, Issue 3, 2011, pp. 577-587.
[20.] Kardas-Cinal, E., Comparative study of running safety and ride comfort of railway vehicle, Prace Naukowe Politechniki Warszawskiej, z. 71 Transport, 2009.
[21.] Sharma, R.C., Parametric analysis of rail vehicle parameters influencing ride behavior, International Journal of Engineering, Science and Technology, Vol. 3, No. 8, 2011, pp. 54-65.
[22.] Zhou, J., Goodall, R., Ren, L., Zhang, H., Influences of car body vertical flexibility on ride quality of passenger railway vehicles, Proceedings of the Institution of Mechanical Engineers, Part F: Journal of Rail and Rapid Transit, Vol. 223, 2009, pp. 461-471.
[23.] Sun,W., Gong, D., Zhou, J., Zhao Z., Influences of suspended equipment under car body on highspeed train ride quality, Procedia Engineering, Vol. 16, 2011, pp. 812 – 817.
[24.] Dumitriu, M., Evaluation of the comfort index in railway vehicles depending on the vertical suspension features, Annals of Faculty Engineering Hunedoara – International Journal of Engineering, Tome XI, Fascicule 4, 2013, pp. 23-32.
[25.] Dumitriu, M., Influence of damping suspension on the vibration eigenmodes of railway vehicles, Mechanical Journal Fiability and Durability, Iss. 1, 2013, pp. 109 – 115.
[26.] Förstberg, J., Ride comfort and motion sickness in tilting trains. Human responses to motion environments in train experiment and simulator experiments, Doctoral thesis. Railway Technology Department of Vehicle Engineering Royal Institute of Technology, Stockholm, 2000.
[27.] Kim, Y.G., Kwon, H.B., Kim, S.W., Park, C.K. Park, T.W., Correlation of ride comfort evaluation methods for railway vehicles, Proceedings of the Institution of Mechanical Engineers, Part F: Journal of Rail and Rapid Transit, Vol. 217, 2003, pp. 73-88.
[28.] Enblom, R., Two-level numerical optimization of ride comfort in railway vehicles, Proceedings of the Institution of Mechanical Engineers, F: Journal of Rail and Rapid Transit, Vol. 220, 2006, pp. 1-16.
[29.] Schandl, G., Lugner, P., Benatzky, C., Kozek, M., Stribersk, M., Comfort enhancement by an active vibration reduction system for a flexible railway car body, Vehicle System Dynamics Vol. 45, No. 9, 2007, pp. 835–847.
[30.] Dumitriu, M., On the assessment of the vertical vibration behaviour of a railway vehicle, Romanian Journal of Acoustics and Vibration, Vol. VIII, Iss. 2, 2011, pp. 131-138.
[31.] Dumitriu, M., Considerations on the excitation mechanism of the vertical vibration symmetrical and antisymmetrical modes in railway vehicles, Annals of the University of Petroşani, Mechanical Engineering, Vol. 15, 2013, pp. 58-71.
[32.] Dumitriu, M., Considerations on the geometric filtering effect of the bounce and pitch movements in railway vehicles, Annals of Faculty Engineering Hunedoara – International Journal of Engineering, Tome XII, Fascicule 3, 2014, pp. 155-164
[33.] ORE B 176/1989. Bogies with steered or steering wheelsets, Report No. 1: Specifications and preliminary studies, Vol. 2. Specification for a bogie with improved curving characteristics.